Commun. Theor. Phys. **77** (2025) 085801 (9pp)
https://doi.org/10.1088/1572-9494/adb5f4
CSTR: 32041.14.CTP.adb5f4

A map neuron with a hybrid ion channel and its dynamics

Xinlin Song[1], **Ya Wang**[2] **and Feifei Yang**[3]

[1] College of Science, Xi'an University of Science and Technology, Xi'an 710054, China
[2] School of Cyber Security, Gansu University of Political Science and Law, Lanzhou 730070, China
[3] College of Computer Science and Technology, Xi'an University of Science and Technology, Xi'an 710054, China

E-mail: dlpuyff@sina.com

Received 24 November 2024, revised 9 January 2025
Accepted for publication 14 February 2025
Published 14 April 2025

Abstract

The ion channel in neurons is the basic component of signal transmission in the nervous system. The ion channel has important effects on the potential of neuron release and dynamic behavior in neural networks. Ion channels control the flow of ions into and out of the cell membrane to form an ion current, which makes the excitable membrane produce special potential changes and become the basis of nerve and muscle activity. The blockage of ion channels has a significant effect on the dynamics of neurons and networks. Therefore, it is very meaningful to study the influence of ion channels on neuronal dynamics. In this work, a hybrid ion channel is designed by connecting a charge-controlled memristor (CCM) with an inductor in series, and a magnetic flux-controlled memristor (MFCM), capacitor, and nonlinear resistor are connected in parallel with the mixed ion channel to obtain the memristor neural circuit. Furthermore, the oscillator model with a hybrid ion channel and its energy function are calculated, and a map neuron is obtained by linearizing the neuron oscillator model. In addition, an adaptive regulation method is designed to explore the adaptive regulation of energy on the dynamic behaviors of the map neuron. The results show that the dynamics of a map neuron with a hybrid ion channel can be controlled by parameters and external magnetic fields. This study is also used to research synchronization between map neurons and collective behaviors in the map neurons network.

Keywords: map neuron, hybrid ion channel, dynamical behaviors, adaptive regulation

(Some figures may appear in colour only in the online journal)

1. Introduction

The memristor is a two-terminal passive circuit electronic element with unique memory properties. Its resistance state changes with the amount of charge passed through, and it is able to 'remember' these changes [1]. Due to the unique characteristics of memristors, they are widely used in the fields of memory, logic, analog circuits, and neuromorphic systems. A magnetic flux-controlled memristor (MFCM) [2–6] and a charge-controlled memristor (CCM) [7–11] are two different realization methods based on the concept of a memristor, and they have their own characteristics in circuit design, dynamic characteristics, and application fields.

MFCM is defined based on the relationship between magnetic flux and resistance, and its working principle involves the effect of magnetic flux changes in the circuit on the resistance value. The research and application of MFCM mainly focuses on the design and simulation of chaotic circuits. For example, chaotic systems designed by MFCM can produce complex dynamic behaviors such as hidden attractors [12–14], coexisting attractors [15], multi-scroll attractors [16–19], and multi-stable [20–24]. CCM memristor is defined based on the relationship between charge and resistance, and its working principle involves the effect of the change of charge in the circuit on the resistance value. The research and application of CCM is also extensive, such as the design of chaotic circuits [25, 26], the design of the memristor simulator, the application of memristors in memory, neural networks, and other fields

The memristor has the characteristics of memory and non-volatility. Therefore, memristors can simulate brain

synapses, and they can be used to construct neural networks based on memristors. These networks not only inherit the advantages of low power consumption and nano size of memristors but they also contribute to improving the performance of neural networks. There is plenty of research on memristor applications in neurons, synapses, and networks. For example, memristive neurons [27–32], dual memristors neurons [33, 34], memristive map neurons [35–38], neurons with memristive membrane [39–41] synchronizing characteristics of memristive synapse coupling neurons [42–45], collective behaviors of memristive neuron network [46, 47], the learning in memristor networks [48, 49]. With the research on memristor-based neurons and networks, readers can read the reviews [50].

The change in resistance of the memristor can lead to a change in resistance state through ion transport, a process similar to the opening and closing mechanism of ion channels in biological neurons. Therefore, the memristor can be considered to describe ion channels in the neurons. In this work, a hybrid ion channel is built by connecting a CCM with an inductor in series, and an MFCM, capacitor, and nonlinear resistor are connected in parallel with the mixed ion channel to obtain the memristor neural circuit. Furthermore, the oscillator model with a hybrid ion channel and its energy function are calculated, and a map neuron is obtained by linearizing the neuron oscillator model. The highlights and contributions of this study are summarized as follows:

(1) A hybrid ion channel is built by connecting a CCM with an inductor in series
(2) A map neuron with a hybrid ion channel is obtained by linearizing the neuron oscillator model.
(3) An adaptive regulation method based on energy is designed.

The structure of this study is arranged as follows: the model of map neuron with a hybrid ion channel is built in section 2. In section 3, the dynamical behaviors of the map neuron are estimated. The conclusion is described in section 4.

2. Model of map neuron

The activation and deactivation characteristics of neuron ion channels can be affected by the electric and magnetic fields, and the firing activity and network behavior of neurons are regulated by changing the distribution and flow of ions. Therefore, in this paper, a hybrid ion channel of a neuron is built by connecting an induction coil with a CCM in series for estimating the effects of electric and magnetic fields on ion channels. A neural circuit with a hybrid ion channel is shown in figure 1.

The neural circuit with a hybrid ion channel is designed by applying a capacitor (C), an inductor (L), a nonlinear resistor (R_N), a linear resistor (R), a CCM, and an MFCM. In figure 1, the current i_N in the R_N is approached by

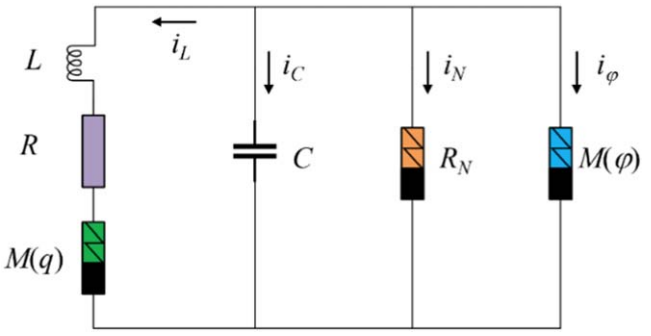

Figure 1. A nonlinear circuit with a hybrid ion channel.

$$i_N = -\frac{r}{\rho}\left(V - \frac{V^2}{V_0}\right), \tag{1}$$

where ρ and V_0 denote the resistance and the cut-off voltage in the nonlinear resistor R_N. In addition, a CCM and an MFCM can be selected as follows

$$\begin{cases} V_M = M(q)i_M = qi_M, \dfrac{\mathrm{d}q}{\mathrm{d}t} = \alpha q + \beta i_M \\ i_\varphi = M(\varphi)V_\varphi = \varphi V_\varphi, \dfrac{\mathrm{d}\varphi}{\mathrm{d}t} = a\varphi + bV_\varphi \end{cases}, \tag{2}$$

where (α, β, a, b) are the relevant parameters for preparing memristor material. (i_M, V_M, i_φ, V_φ) denote the current and voltage in the memristor. The equivalent dynamic model in figure 1 is obtained by using the Kirchhoff's laws, and it is presented as

$$\begin{cases} C\dfrac{\mathrm{d}V}{\mathrm{d}t} = -i_L + \dfrac{r}{\rho}\left(V - \dfrac{V^2}{V_0}\right) - \varphi V \\ L\dfrac{\mathrm{d}i_L}{\mathrm{d}t} = V - qi_M - Ri_L \\ \dfrac{\mathrm{d}q}{\mathrm{d}t} = \alpha q + \beta i_M \\ \dfrac{\mathrm{d}\varphi}{\mathrm{d}t} = a\varphi + bV_\varphi \end{cases}. \tag{3}$$

To further numerical simulation, the variables in equation (3) are replaced as follows

$$x = \frac{V}{V_0}; y = \frac{\rho i_L}{V_0}; z = \frac{q}{CV_0}; w = \frac{\varphi}{\rho CV_0}; \tau = \frac{t}{\rho C}. \tag{4}$$

As a result, the model in equation (3) can be expressed by

$$\begin{cases} \dfrac{\mathrm{d}x}{\mathrm{d}\tau} = -y + r(x - x^2) - cwx \\ \dfrac{\mathrm{d}y}{\mathrm{d}\tau} = d(x - ezy - gy) \\ \dfrac{\mathrm{d}z}{\mathrm{d}\tau} = \alpha' z + \beta y \\ \dfrac{\mathrm{d}w}{\mathrm{d}\tau} = a'w + bx \end{cases}, \tag{5}$$

where parameters in equation (5) are defined as follows

$$c = \rho^2 C V_0;\ d = \frac{\rho^2 C}{L};\ e = \frac{CV_0}{\rho};$$
$$g = \frac{R}{\rho};\ \alpha' = \rho\alpha C;\ a' = a\rho C. \tag{6}$$

The circuit in figure 1 has four energy storage elements, and the corresponding field energy can be approached by

$$W = W_C + W_L + W_M + W_\varphi$$
$$= \frac{1}{2}CV^2 + \frac{1}{2}Li_L^2 + \frac{1}{2}q^2 i_L + \frac{1}{2}\varphi^2 V. \tag{7}$$

Furthermore, the dimensionless Hamilton energy is calculated as follows

$$H = \frac{W}{CV_0^2} = H_C + H_L + H_M + H_\varphi$$
$$= \frac{1}{2}x^2 + \frac{1}{2d}y^2 + \frac{1}{2}ez^2 y + \frac{1}{2}cw^2 x. \tag{8}$$

In fact, the energy function in equation (8) is also obtained by applying the Helmholtz's theorem, the process is described in the following.

$$\begin{pmatrix}\dot{x}\\ \dot{y}\\ \dot{z}\\ \dot{w}\end{pmatrix} = \begin{pmatrix}-y + r(x - x^2) - cwx\\ d(x - ezy - gy)\\ \alpha' z + \beta y\\ a' w + bx\end{pmatrix} = F_c + F_d$$

$$= \begin{pmatrix}-y - 0.5dez^2 - cwx\\ dx + 0.5cdw^2 - de\beta zy\\ \beta y + 0.5de\beta z^2\\ x + 0.5cw^2\end{pmatrix}$$

$$+ \begin{pmatrix}r(x - x^2) + 0.5dez^2\\ dezy(\beta - 1) - dgy + 0.5cdw^2\\ \alpha' z - 0.5de\beta z^2\\ (b - 1)x + a' w - 0.5cw^2\end{pmatrix}$$

$$= \begin{pmatrix}0 & -d & 0 & -1\\ d & 0 & -\beta d & 0\\ 0 & \beta d & 0 & 0\\ 1 & 0 & 0 & 0\end{pmatrix}\begin{pmatrix}x + 0.5cw^2\\ y/d + 0.5ez^2\\ ezy\\ cwx\end{pmatrix}$$

$$+ \begin{pmatrix}n_1 & 0 & 0 & 0\\ 0 & n_2 & 0 & 0\\ 0 & 0 & n_3 & 0\\ 0 & 0 & 0 & n_4\end{pmatrix}\begin{pmatrix}x + 0.5cw^2\\ y/d + 0.5ez^2\\ ezy\\ cwx\end{pmatrix}, \tag{9}$$

where

$$\begin{cases} n_1 = \dfrac{r(x - x^2) + 0.5dez^2}{x + 0.5cw^2};\ n_2 = \dfrac{dezy(\beta - 1) - dgy + 0.5cdw^2}{y/d + 0.5ez^2} \\ n_3 = \dfrac{\alpha' z - 0.5de\beta z^2}{ezy};\ n_4 = \dfrac{(b - 1)x + a' w - 0.5cw^2}{cwx} \end{cases}. \tag{10}$$

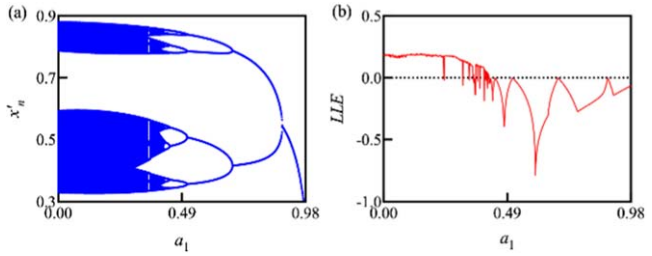

Figure 2. Bifurcation diagram and *LLE* with different parameter a_1. For (a) bifurcation diagram for parameter a_1; (b) *LLE* for parameter a_1.

In fact, the energy function in equation (8) needs to meet equation (11).

$$\nabla H^T F_c = 0;\ \nabla H^T F_d = \frac{\partial H}{d\tau}. \tag{11}$$

The energy function in equation (8) can be obtained by solving the solution in the following equation.

$$\nabla H^T F_c = (-y - 0.5dez^2 - cwx)\frac{\partial H}{\partial x}$$
$$+ (dx + 0.5cdw^2 - de\beta zy)\frac{\partial H}{\partial y}$$
$$+ (\beta y + 0.5de\beta z^2)\frac{\partial H}{\partial z}$$
$$+ (x + 0.5cw^2)\frac{\partial H}{\partial w} = 0. \tag{. 12}$$

A suitable solution in equation (12) is the energy function in equation (8). In a genetic way, the oscillator model can be transformed into a discrete form using the Euler difference algorithm. However, this discretization process introduces a time step parameter, the value of which significantly influences the dynamics of the resulting map. Therefore, a linear transformation combined with the time step is employed to establish a set of new discrete variables and parameters. Furthermore, the variables in equation (5) are linearly transformed by

$$x'_n = \frac{r\Delta\tau}{1 + r\Delta\tau}x_n;\ y'_n = \frac{r\Delta\tau}{1 + r\Delta\tau}y_n;$$
$$z'_n = \frac{r\Delta\tau}{1 + r\Delta\tau}z_n;\ w'_n = \frac{r\Delta\tau}{1 + r\Delta\tau}w_n, \tag{13}$$

where $\Delta\tau$ denotes the time step in equation (5), as a result, a map neuron can be obtained as follows

$$\begin{cases} x'_{n+1} = -\lambda_1 y'_n + r_1(x'_n - {x'_n}^2) - c_1 w'_n x'_n \\ y'_{n+1} = d_1(x'_n - e_1 z'_n y'_n - g_1 y'_n) \\ z'_{n+1} = \alpha_1 z'_n + \beta_1 y'_n \\ w'_{n+1} = a_1 w'_n + b_1 x'_n \end{cases}, \tag{14}$$

where the parameters in equation (14) are defined by

$$\begin{cases} \lambda_1 = \Delta\tau;\ r_1 = 1 + r\Delta\tau;\ c_1 = c\dfrac{1 + r\Delta\tau}{r};\ d_1 = d\Delta\tau;\ e_1 = e\dfrac{1 + r\Delta\tau}{r\Delta\tau}; \\ g_1 = g - \dfrac{1}{d\Delta\tau};\ \alpha_1 = 1 + \alpha'\Delta\tau;\ \beta_1 = \beta\Delta\tau;\ a_1 = 1 + a'\Delta\tau;\ b_1 = b\Delta\tau. \end{cases}. \tag{15}$$

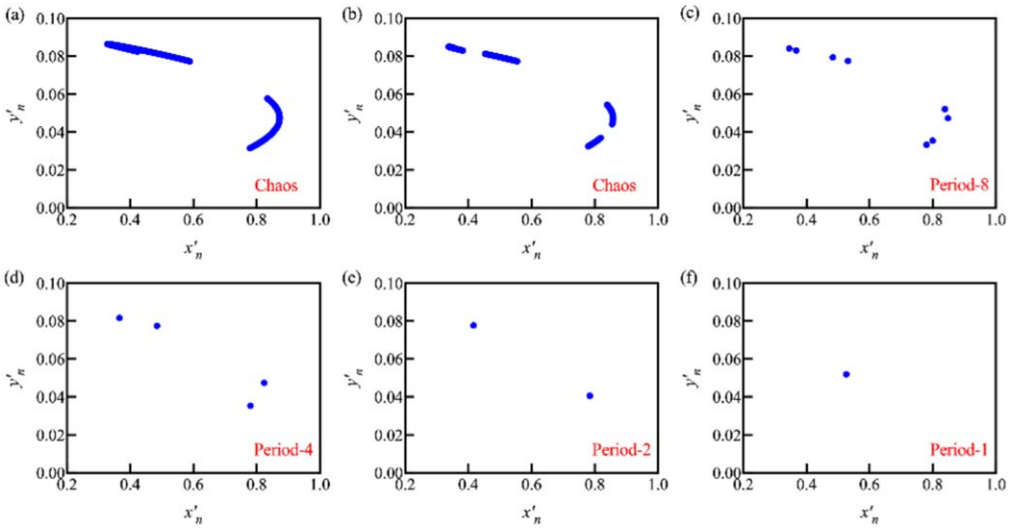

Figure 3. Attractor phase of the map neuron with different parameter a_1. For (a) $a_1 = 0.2$; (b) $a_1 = 0.392$; (c) $a_1 = 0.47$; (d) $a_1 = 0.6$; (e) $a_1 = 0.7$; (f) $a_1 = 0.9$.

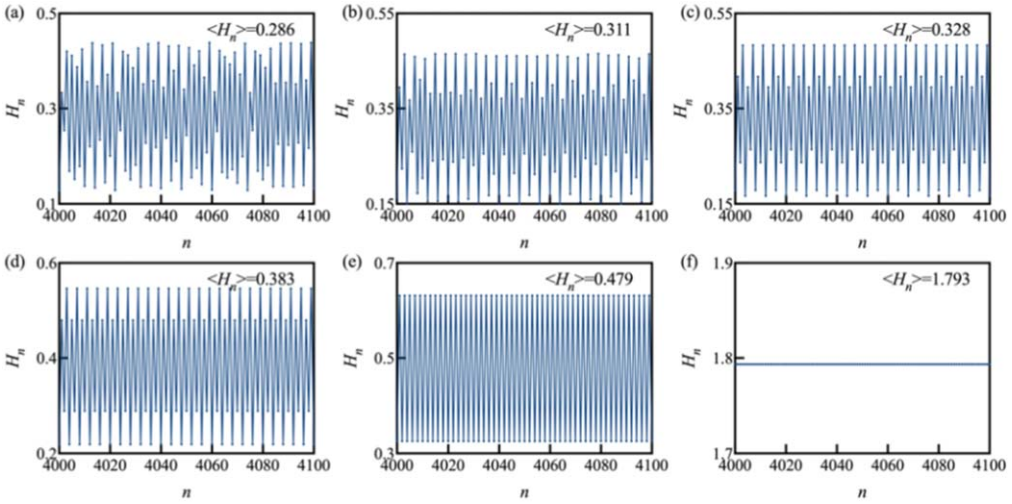

Figure 4. Evolution of H_n for different parameter a_1. For (a) $a_1 = 0.2$; (b) $a_1 = 0.392$; (c) $a_1 = 0.47$; (d) $a_1 = 0.6$; (e) $a_1 = 0.7$; (f) $a_1 = 0.9$. $<H_n>$ is a mean value of energy within 100 iterations.

Similarly, the energy function in equation (8) is updated as follows

$$H_n = \frac{1}{2}x'^2_n + \frac{1}{2d_1}y'^2_n + \frac{1}{2}e_1 z'^2_n\, y'_n + \frac{1}{2}c_1 w'^2_n\, x'_n. \qquad (16)$$

3. Numerical simulation estimations

The dynamic of the map neuron in equation (14) is estimated by using the numerical simulation with the iterative method on the MATLAB. At first, parameters of the map neuron with a hybrid ion channel are set at $r_1 = 3.8$, $c_1 = 0.1$, $d_1 = 0.1$, $e_1 = 3.6316$, $g_1 = 0.1$, $\alpha_1 = 0.1$, $\beta_1 = 0.2$, $\lambda_1 = 0.1$, and its initial value is (0.01, 0.1, 0.1, 0.1). For parameter $b_1 = 1.5$, a_1 is changed from 0 to 0.98, the largest Lyapunov exponent (*LLE*) and bifurcation diagram can be obtained, and the results are shown in figure 2.

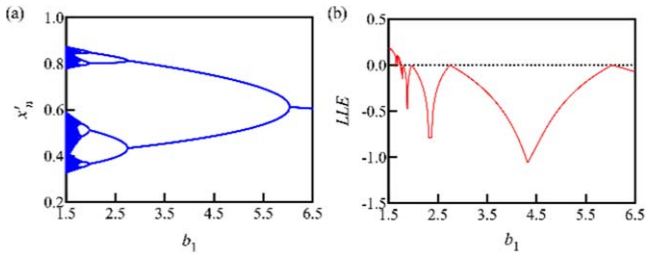

Figure 5. Bifurcation diagram and *LLE* with different parameter b_1. For (a) bifurcation diagram for parameter b_1; (b) *LLE* for parameter b_1.

The dynamic in figure 2 shows that the map neuron with a hybrid ion channel evolves from a chaotic state to a periodic state by period-doubling bifurcation in the process of parameter enlargement. Furthermore, the phase portraits with different states are shown in figure 3.

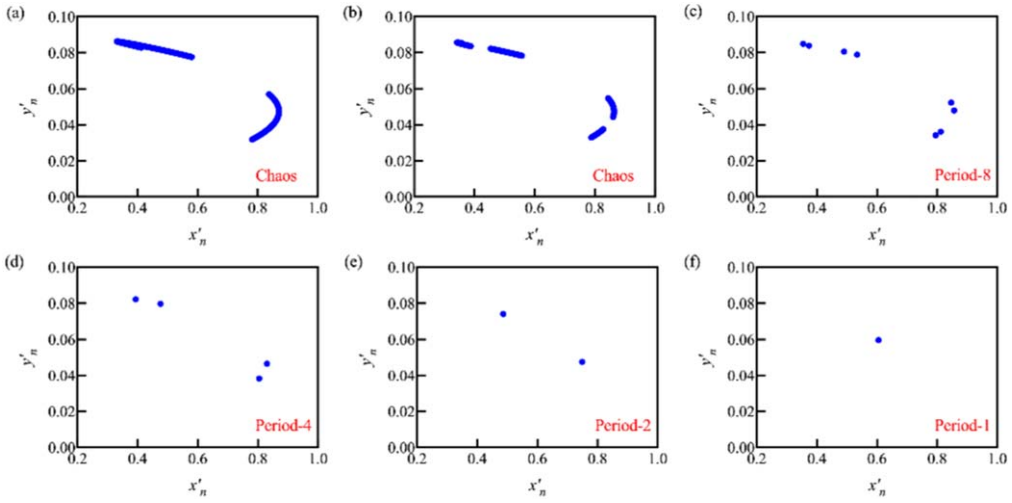

Figure 6. Phase portraits of the map neuron for different parameter b_1. For (a) $b_1 = 1.55$; (b) $b_1 = 1.7$; (c) $b_1 = 1.88$; (d) $b_1 = 2.5$; (e) $b_1 = 4.5$; (f) $b_1 = 6.5$. $a_1 = 0.2$.

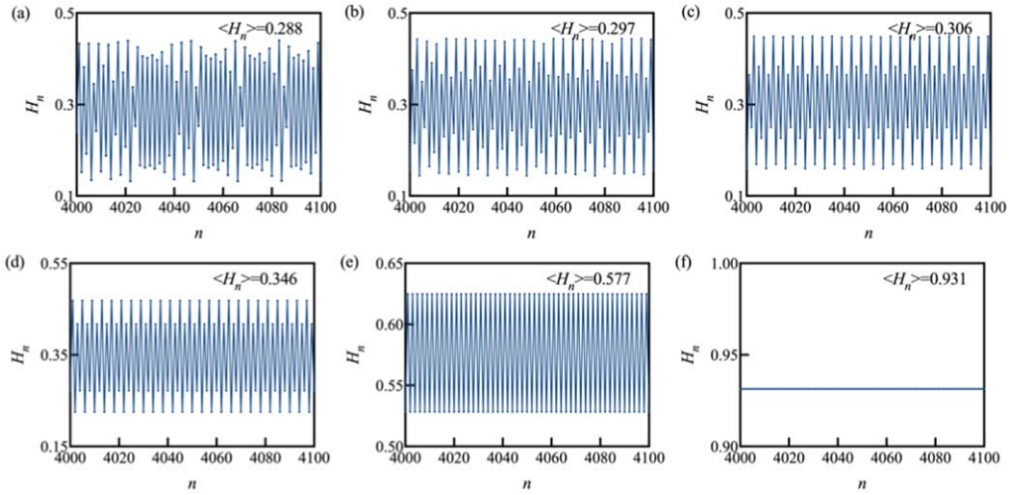

Figure 7. Evolution of H_n for different parameter b_1. For (a) $b_1 = 1.55$; (b) $b_1 = 1.7$; (c) $b_1 = 1.88$; (d) $b_1 = 2.5$; (e) $b_1 = 4.5$; (f) $b_1 = 6.5$; Setting $a_1 = 0.2$. $<H_n>$ is a mea$_n$ energy value within 100 iterations.

Figure 3 illustrates that the different attractors can be formed by adjusting parameter a_1, such as chaotic patterns, period-8, period-4, period-2 and period-1 states. In figure 4, according to the energy function in equation (16), the evolution of energy with different dynamic behaviors in figure 3 is obtained in figure 4.

The result in figure 4 indicates that the chaotic map neuron keeps a lower average value of energy, while the period map neuron has a higher mean energy value. Especially, when the number of the periodic is further decreased, the value of the $<H_n>$ can be increased. Similarly, parameter $a_1 = 0.2$, the effect of parameter b_1 on the dynamical characteristics of the map neuron in equation (14) is discussed. Parameters and initial value in the map neuron are kept as above, and the results are displayed in figure 5.

Similar to the results of the case of parameter a_1, parameter b_1 is increased, chaotic modes of the map neuron with a hybrid ion channel will show the periodic patterns. Furthermore, the phase diagrams of a map neuron with different parameter b_1 are plotted in figure 6.

It is found that the chaotic and periodic attractors can be developed by changing parameter b_1. Figure 7 displayed the evolution of energy with different parameter values of b_1.

Similarly, the number of the periodic is further decreased, the value of $<H_n>$ can be increased. To research the influence of external magnetic fields on the nonlinear behaviors of a map neuron, the map neuron with a hybrid ion channel can be presented as follows

$$\begin{cases} x'_{n+1} = -\lambda_1 y'_n + r_1(x'_n - x'^2_n) - c_1 w'_n x'_n \\ y'_{n+1} = d_1(x'_n - e_1 z'_n y'_n - g_1 y'_n) \\ z'_{n+1} = \alpha_1 z'_n + \beta_1 y'_n \\ w'_{n+1} = a_1 w'_n + b_1 x'_n + \varphi_{ext} \end{cases}, \quad (17)$$

where φ_{ext} is the external magnetic field. In this case, the bifurcation diagram of the map neuron in (17) with different

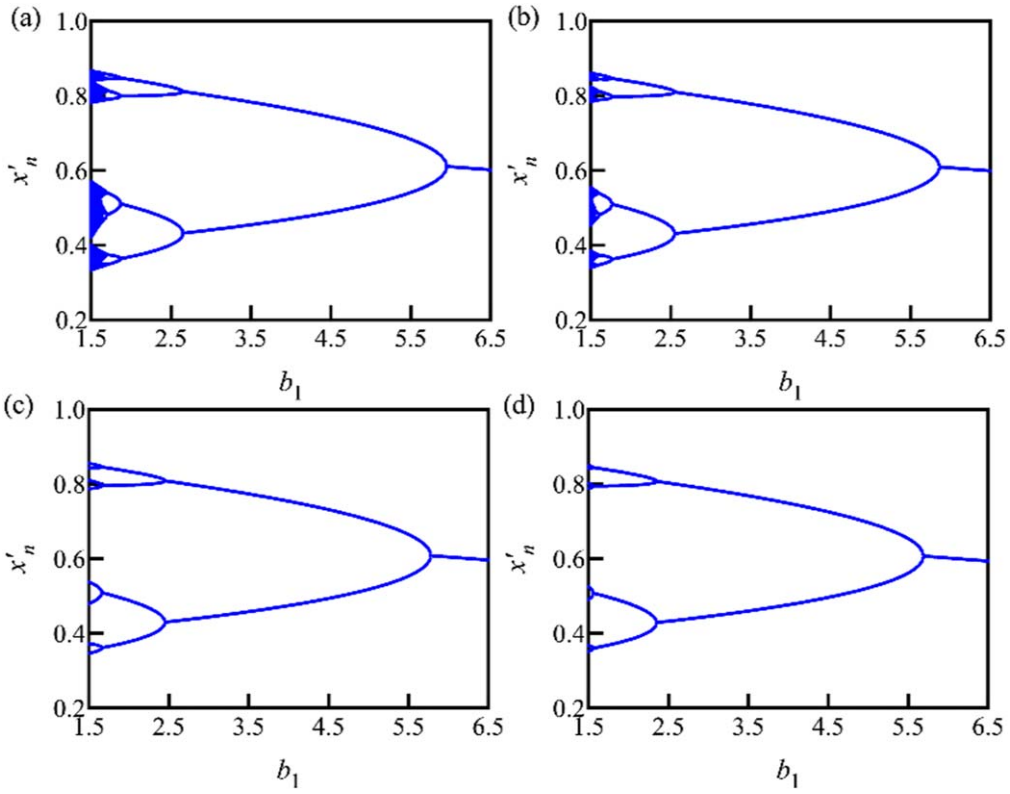

Figure 8. Bifurcation diagram of the map neuron in equation (17) by changing parameter b_1 under different φ_{ext}. For (a) $\varphi_{ext} = 0.1$; (b) $\varphi_{ext} = 0.2$; (c) $\varphi_{ext} = 0.3$; (d) $\varphi_{ext} = 0.4$.

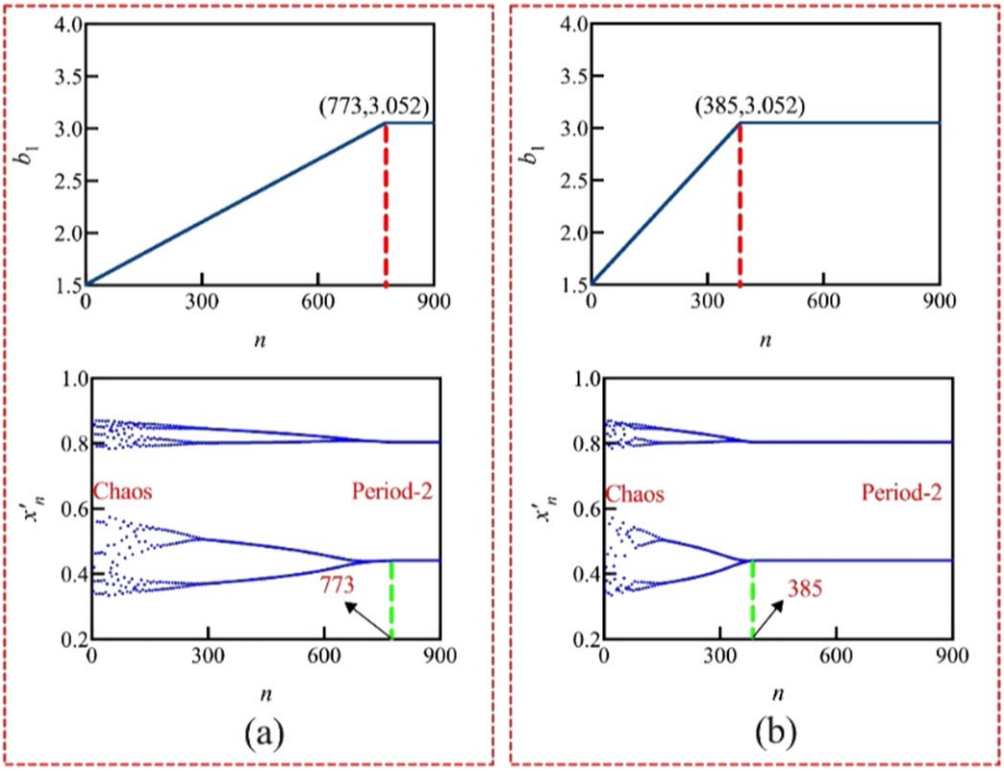

Figure 9. Evolution of parameter b_1 and variable x'_n. For (a) $\kappa_0 = 0.004$; (b) $\kappa_0 = 0.008$.

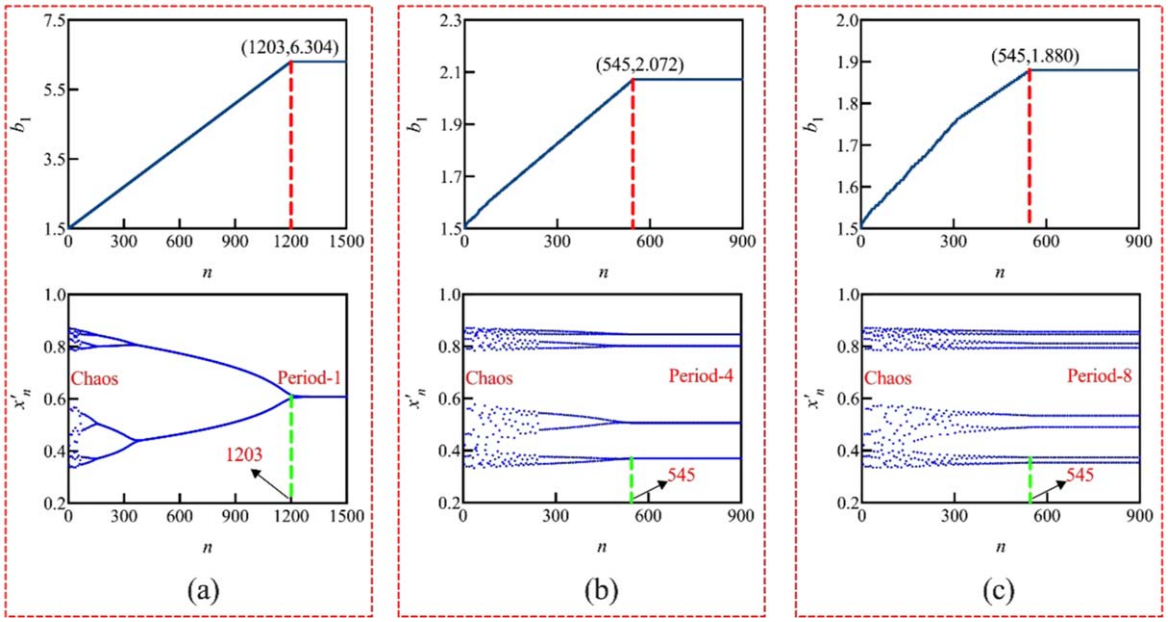

Figure 10. Evolution of parameter b_1 and variable x'_n. For (a) $\varepsilon = 0.9$; (b) $\varepsilon = 0.18$; (c) $\varepsilon = 0.16$.

parameter $b1$ under different φ_{ext} is calculated. The parameter and initial value are kept as above, and the results are displayed in figure 8.

Figure 8 shows that the nonlinear behavior of a map neuron with a hybrid ion channel can be controlled by the magnetic fields. In addition, the strength of the magnetic field is increased, the chaotic states of a map neuron can be suppressed and the periodic states induced. In addition, to analyze adaptive regulation of the energy on the nonlinear behavior of the map neuron, an adaptive growth method of parameter can be designed as follows

$$\begin{cases} b_1(n+1) = b_1(n) + \kappa_0 \cdot \theta(\varepsilon - H_n), \\ \theta(P) = 1,\ P \geqslant 0,\ \theta(P) = 0,\ P < 0, \end{cases} \tag{18}$$

where (κ_0, ε) denote the gain and energy threshold, the Heaviside function θ can control parameter b_1. The initial value for the parameter b_1 is 1.5, $a_1 = 0.2$, $\varepsilon = 0.306$, the other parameters and initial value remain as above, the evolution of parameter b_1 and the variable with different gain is a gain κ_0 is as shown in figure 9.

The results in figure 9 illustrate that the chaotic map neuron can be controlled to period-2 patterns by the adaptive growth method in equation (18), and parameter b_1 is also to reach a stable value. The gain is increased, and the parameter reaches a stable value in fewer iterations. Furthermore, the gain $\kappa_0 = 0.004$, the case of the different threshold ε is figure 10.

Figure 10 shows that the chaotic map neuron can be developed to different periodic states by applying an energy threshold to control the parameter b_1. In fact, the other parameters in the map neuron with a hybrid ion channel can be also used to research the adaptive regulation.

4. Conclusion

In this paper, a hybrid ion channel is obtained by connecting a CCM with an inductor in series, and an MFCM, capacitor and nonlinear resistor are connected in parallel with the mixed ion channel to obtain the memristor neural circuit. Furthermore, the oscillator model with a hybrid ion channel and its energy function are calculated, and a map neuron is obtained by linearizing the neuron oscillator model. The results illustrate that the map neuron with a hybrid ion channel evolve from a chaotic state to a periodic state by period-doubling bifurcation in the process of parameter enlargement, and the chaotic map neuron keeps a lower average value of energy, while the period map neuron has a higher mean energy value. Especially, when the number of the periodic is further decreased, the value of the $<H_n>$ can be increased. The nonlinear behavior of a map neuron with a hybrid ion channel is controlled by the magnetic fields. Furthermore, the chaotic map neuron can be controlled to period-2 patterns by the adaptive growth method, and the chaotic map neuron can be developed to different periodic states by applying an energy threshold to control the parameter. This study is helpful for building an ion channel of the Artificial neuron.

Acknowledgments

This research is supported by the National Science Basic Research Program of Shaanxi (Grant No. 2023-JC-QN-0087).

Authorship contribution statement

XS: Writing-original draft, formal analysis, investigation. **YW:** Numerical. **FY:** Methodology, formal analysis, investigation, writing-final version.

Declaration of competing interest

There are no competing interests in this study.

References

[1] Chua L 1971 Memristor-The missing circuit element *IEEE Trans. Circuit Theory* **18** 507–19

[2] Batas D and Fiedler H 2011 A memristor SPICE implementation and a new approach for magnetic flux-controlled memristor modeling *IEEE Trans. Nanotechnol.* **10** 250–5

[3] Li C, Yang Y, Du J and Chen Z 2021 A simple chaotic circuit with magnetic flux-controlled memristor *Eur. Phys. J. Speéc. Top.* **230** 1723–36

[4] Wu H-G, Bao B-C and Chen M 2014 Threshold flux-controlled memristor model and its equivalent circuit implementation *Chin. Phys.* B **23** 118401

[5] Zhu J, Cao Y, Mou J and Banerjee S 2024 KTz neuron in electromagnetic radiation with a novel flux-controlled memristor *Int. J. Bifurc. Chaos* **34** 2450140

[6] Min F, Cheng Y, Lu L and Li X 2021 Extreme multistability and antimonotonicity in a shinriki oscillator with two flux-controlled memristors *Int. J. Bifurc. Chaos* **31** 2150167

[7] Si G, Diao L and Zhu J 2016 Fractional-order charge-controlled memristor: theoretical analysis and simulation *Nonlinear Dyn.* **87** 2625–34

[8] Fouda M E and Radwan A G 2012 Charge controlled memristor-less memcapacitor emulator *Electron. Lett.* **48** 1454–5

[9] Chandía K J, Bologna M and Tellini B 2018 Multiple scale approach to dynamics of an LC circuit with a charge-controlled memristor *IEEE Trans. Circuits Syst. II: Express Briefs* **65** 120–4

[10] Sun J, Yang J, Liu P and Wang Y 2023 Design of general flux-controlled and charge-controlled memristor emulators based on hyperbolic functions *IEEE Trans. Comput.-Aided Des. Integr. Circuits Syst.* **42** 956–67

[11] Isah A, Nguetcho A S T, Binczak S and Bilbault J M 2020 Dynamics of a charge-controlled memristor in master–slave coupling *Electron. Lett.* **56** 211–3

[12] Huang L, Wang Y, Jiang Y and Lei T 2021 A novel memristor chaotic system with a hidden attractor and multistability and its implementation in a circuit *Math. Probl. Eng.* **2021** 7457220

[13] Dong C and Yang M 2024 Extreme homogeneous and heterogeneous multistability in a novel 5D memristor-based chaotic system with hidden attractors *Fractal Fract.* **8** 266

[14] Zhao G, Zhao H, Zhang Y and An X 2024 A new memristive system with extreme multistability and hidden chaotic attractors and with application to image encryption *Int. J. Bifurc. Chaos* **34** 2450010

[15] Wang Q, Hu C, Tian Z, Wu X, Sang H and Cui Z 2024 A 3D memristor-based chaotic system with transition behaviors of coexisting attractors between equilibrium points *Res. Phys.* **56** 107201

[16] Ma J, Zhou P, Ahmad B, Ren G and Wang C 2018 Chaos and multi-scroll attractors in RCL-shunted junction coupled Jerk circuit connected by memristor *PLoS One* **13** e0191120

[17] Li J, Wang C and Deng Q 2024 Symmetric multi-double-scroll attractors in Hopfield neural network under pulse controlled memristor *Nonlinear Dyn.* **112** 14463–77

[18] Ding R, Bao H, Wang N, Wu H and Xu Q 2024 Generating multi-scroll chaotic attractor in a three-dimensional memristive neuron model *Chin. J. Phys.* **88** 1053–67

[19] Tang D, Wang C, Lin H and Yu F 2024 Dynamics analysis and hardware implementation of multi-scroll hyperchaotic hidden attractors based on locally active memristive Hopfield neural network *Nonlinear Dyn.* **112** 1511–27

[20] Zhang L, Li Z and Peng Y 2024 A hidden grid multi-scroll chaotic system coined with two multi-stable memristors *Chaos, Solitons Fractals* **185** 115109

[21] Zhang J and Wang X 2024 Design and implement a nested coexisting multi-vortex hyperchaotic system with multiple stability memristors *Phys. Scr.* **99** 105213

[22] Ma T, Mou J, Al-Barakati A A, Jahanshahi H and Miao M 2023 Hidden dynamics of memristor-coupled neurons with multi-stability and multi-transient hyperchaotic behavior *Phys. Scr.* **98** 105202

[23] Wu H, Bian Y, Zhang Y, Guo Y, Xu Q and Chen M 2023 Multi-stable states and synchronicity of a cellular neural network with memristive activation function *Chaos, Solitons Fractals* **177** 114201

[24] Wang M-J and Gu L 2024 Multiple mixed state variable incremental integration for reconstructing extreme multistability in a novel memristive hyperchaotic jerk system with multiple cubic nonlinearity *Chin. Phys.* B **33** 020504

[25] Wu S, Rong X and Liu Z Study on how to design simplest chaotic circuit with two charge-controlled study on how to design simplest chaotic circuit with two charge-controlled memristors *J. Syst. Sim.* **30** 3985–95

[26] Wang M, Yi Z and Li Z 2025 A memristive Ikeda map and its application in image encryption *Chaos, Solitons Fractals* **190** 115740

[27] Yang F, Xu Y and Ma J 2023 A memristive neuron and its adaptability to external electric field *Chaos: Interdiscip. J. Nonlinear Sci.* **33** 023110

[28] Yang F, Han Z, Ren G, Guo Q and Ma J 2024 Enhance controllability of a memristive neuron under magnetic field and circuit approach *Eur. Phys. J. Plus* **139** 534

[29] Xie Y, Ye Z, Li X, Wang X and Jia Y 2024 A novel memristive neuron model and its energy characteristics *Cogn. Neurodynamics* **18** 1989–2001

[30] Bao B, Zhu Y, Ma J, Bao H, Wu H and Chen M 2021 Memristive neuron model with an adapting synapse and its hardware experiments *Sci. China Technol. Sci.* **64** 1107–17

[31] Lin H, Wang C, Sun Y and Yao W 2020 Firing multistability in a locally active memristive neuron model *Nonlinear Dyn.* **100** 3667–83

[32] Wu F, Hu X and Ma J 2022 Estimation of the effect of magnetic field on a memristive neuron *Appl. Math. Comput.* **432** 127366

[33] Shen H, Yu F, Wang C, Sun J and Cai S 2022 Firing mechanism based on single memristive neuron and double memristive coupled neurons *Nonlinear Dyn.* **110** 3807–22

[34] Yang F, Ren G and Tang J 2023 Dynamics in a memristive neuron under an electromagnetic field *Nonlinear Dyn.* **111** 21917–39

[35] Jia J, Wang C, Zhang X and Zhu Z 2024 Energy and self-adaption in a memristive map neuron *Chaos, Solitons Fractals* **182** 114738

[36] Yang F, Song X and Ma J 2024 A memristive map neuron under noisy electric field *Chin. J. Phys.* **91** 287–98

[37] Li Y, Lv M, Ma J and Hu X 2024 A discrete memristive neuron and its adaptive dynamics *Nonlinear Dyn.* **112** 7541–53

[38] Wang B, Zhang X, Zhu Z and Ren G 2024 A new memristive map neuron, self-regulation and coherence resonance *Eur. Phys. J.* B **97** 124

[39] Guo Y, Wu F, Yang F and Ma J 2023 Physical approach of a neuron model with memristive membranes *Chaos: Interdiscip. J. Nonlinear Sci.* **33** 113106

[40] Yang F, Song X and Yu Z 2024 Dynamics of a functional neuron model with double membranes *Chaos, Solitons Fractals* **188** 115496
[41] Wan J, Wu F, Ma J and Wang W 2024 Dynamics and synchronization of neural models with memristive membranes under energy coupling *Chin. Phys.* B **33** 050504
[42] Xu F, Zhang J, Fang T, Huang S and Wang M 2018 Synchronous dynamics in neural system coupled with memristive synapse *Nonlinear Dyn.* **92** 1395–402
[43] Vivekanandhan G, Natiq H, Merrikhi Y, Rajagopal K and Jafari S 2023 Dynamical analysis and synchronization of a new memristive chialvo neuron model *Electronics* **12** 545
[44] Guo Y, Zhu Z, Wang C and Ren G 2020 Coupling synchronization between photoelectric neurons by using memristive synapse *Optik* **218** 164993
[45] Mehrabbeik M, Jafari S and Perc M 2023 Synchronization in simplicial complexes of memristive Rulkov neurons *Front. Comput. Neurosci.* **17** 1248976
[46] Yang F, Hu X, Ren G and Ma J 2023 Synchronization and patterns in a memristive network in noisy electric field *Eur. Phys. J.* B **96** 80
[47] Yang F, Wang Y and Ma J 2023 Creation of heterogeneity or defects in a memristive neural network under energy flow *Commun. Nonlinear Sci. Numer. Simul.* **119** 107127
[48] Caravelli F and Carbajal J 2018 Memristors for the Curious Outsiders *Technologies* **6** 118
[49] Carbajal J P, Martin D A and Chialvo D R 2022 Learning by mistakes in memristor networks *Phys. Rev.* E **105** 054306
[50] Yang F, Ma J and Wu F 2024 Review on memristor application in neural circuit and network *Chaos, Solitons Fractals* **187** 115361